Biochimie 232 (2025) 105–116

Contents lists available at ScienceDirect

Biochimie

journal homepage: www.elsevier.com/locate/biochi

Structural and functional significance of two conserved lysine residues in acylated sites of *Kingella kingae* RtxA cytotoxin

Humaira Khaliq [a, 1], Adriana Osickova [a, b, 1], Michaela Lichvarova [a, b], Miroslav Sulc [b], Kevin Munoz Navarrete [a], Carlos Espinosa-Vinals [a], Jiri Masin [a], Radim Osicka [a, *]

[a] *Institute of Microbiology of the Czech Academy of Sciences, v.v.i., 142 20, Prague, Czech Republic*
[b] *Faculty of Science, Charles University in Prague, 128 43, Prague, Czech Republic*

A R T I C L E I N F O

Article history:
Received 8 November 2024
Received in revised form
18 December 2024
Accepted 30 December 2024
Available online 31 December 2024

Handling Editor: Xavier Coumoul

Keywords:
Acylation
Bacterial two-hybrid system
Kingella kingae
Pore-forming toxin
Planar lipid membranes
RtxA

A B S T R A C T

Kingella kingae, an emerging pediatric pathogen, secretes the pore-forming toxin RtxA, which has been implicated in the development of various invasive infections. RtxA is synthesized as a protoxin (proRtxA), which gains its biological activity by fatty acylation of two lysine residues (K558 and K689) by the acyltransferase RtxC. The low acylation level of RtxA at K558 (2–23 %) suggests that the complete acylation at K689 is crucial for toxin activity. Using a bacterial two-hybrid system, we show that substitutions of K558, but not K689, partially reduce the interaction of proRtxA with RtxC and that the acyltransferase interacts independently with each acylated site *in vivo*. While substitutions of K558 had no effect on the acylation of K689, substitutions of K689 resulted in an average 40 % increase in the acylation of K558. RtxA mutants monoacylated at either K558 or K689 irreversibly bound to erythrocyte membranes, with binding efficiency corresponding to the extent of lysine acylation. However, these mutants lysed erythrocytes with similarly low efficiency as nonacylated proRtxA and showed only residual overall membrane activity in planar lipid bilayers. Interestingly, despite forming fewer pores, the monoacylated mutants exhibited single-pore characteristics, such as conductance and lifetime, similar to those of intact RtxA. These findings indicate that the acylation at either K558 or K689 is sufficient for the irreversible insertion of RtxA into the membrane, but not for the efficient formation of membrane pores. Alternatively, K558 and K689 *per se* may play a crucial structural role in pore formation, regardless of their acylation status.

1. Introduction

Kingella kingae, a Gram-negative, fastidious, facultatively anaerobic and β-hemolytic coccobacillus of the *Neisseriaceae* family, is a member of the commensal oropharyngeal microbiota of young children. Recent advances in bacteriological culture methods and molecular detection techniques have demonstrated that *K. kingae* is an important invasive pediatric pathogen and a major cause of osteomyelitis and septic arthritis in children. Other invasive diseases caused by *K. kingae* include bacteremia, infective endocarditis, pericarditis, peritonitis, pneumonia, meningitis and ocular infections [1–9].

K. kingae produces the RtxA toxin, which belongs to the RTX (Repeats in ToXin) family of pore-forming toxins secreted by numerous Gram-negative pathogens [10–12]. RtxA has been shown to be cytotoxic to various human cells, suggesting that it may play a significant role in pathogenesis [13]. Indeed, experiments with *K. kingae* and its RtxA-deficient mutant in an infant rat model confirmed that RtxA is a key virulence factor of the bacterium [14]. Like other RTX toxins, RtxA consists of four characteristic regions in its 956 residues-long molecule (Fig. 1A): (i) a pore-forming domain with five α-helices irreversibly embedded in the membrane (residues ~232 to 409); (ii) an acylated segment where the inactive proRtxA protoxin is activated by the acyltransferase RtxC; (iii) a calcium-binding RTX domain containing conserved nonapeptide repeats forming calcium-binding sites (residues ~725 to 815); and (iv) a C-terminal secretion signal recognized by the type I secretion system [12,15–17]. Upon secretion from the bacterial cell, the C-terminal half of RtxA (residues 511–956) interacts

* Corresponding author. Institute of Microbiology of the Czech Academy of Sciences, Czech Republic.
E-mail address: osicka@biomed.cas.cz (R. Osicka).
[1] These authors contributed equally to this work.

https://doi.org/10.1016/j.biochi.2024.12.016

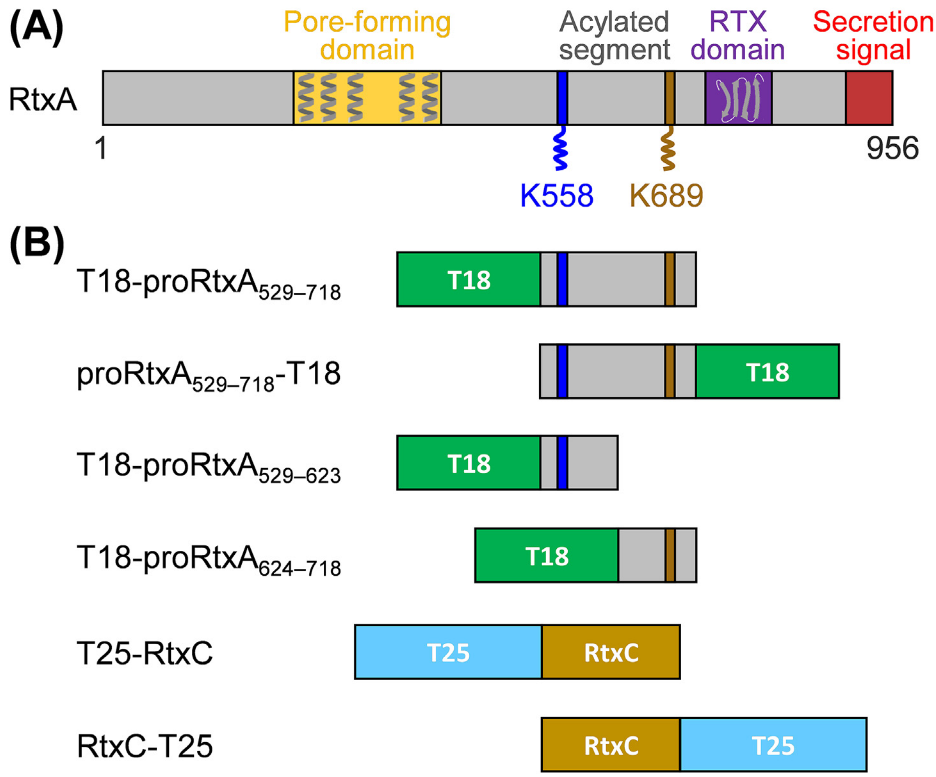

Fig. 1. Schematic representation of RtxA and two-hybrid system fusion variants. (A) RtxA consists of a pore-forming domain, an acylated segment with two acylated lysine residues (K558 and K689), a calcium-binding RTX domain and a C-terminal secretion signal. **(B)** Fusion variants of proRtxA fragments (proRtxA$_{529-718}$, proRtxA$_{529-623}$, proRtxA$_{624-718}$) with T18 and RtxC with T25.

with host cell surfaces primarily via negatively charged sialic acid residues covalently linked to various glycosylated cell surface structures, such as glycoproteins and gangliosides [17–19]. Additionally, membrane cholesterol is crucial for RtxA binding to target cells [15]. Once bound, RtxA inserts into the cell membrane and forms cation-selective pores that induce cation fluxes across the membrane, ultimately leading to cell death [15,20].

The acylated segment of RtxA includes two conserved lysine residues, K558 and K689, which are covalently modified by fatty acyl chains at their ε-amino group by the co-expressed acyltransferase RtxC [15,16]. Mass spectrometry (MS) analysis of recombinant RtxA produced together with RtxC in *Escherichia coli* revealed that the K689 residue is acylated by saturated myristoyl (C14:0) and hydroxymyristoyl (C14:0-OH) chains in 89–91 % of the toxin molecules, while the remaining molecules are modified by lauroyl (C12:0), palmitoyl (C16:0) and palmitoleyl (C16:1) chains. Similarly, the K558 residue is predominantly modified by the C14:0 and C14:0-OH chains, but only in a small proportion of the RtxA molecules, ranging from 2 to 23 %, depending on the toxin batch. This indicates that the extent of the acylation of K558 may vary depending on the physiological state of the bacteria producing the toxin [15,16] and that *in vivo* RtxC preferentially acylates K689. The C14:0 and C14:0-OH chains were also found to be the dominant acyl forms of another RTX toxin, the α-hemolysin HlyA of *E. coli*, which is acylated by the HlyC acyltransferase at residues K564 and K690 [16,21]. In contrast, the RTX adenylate cyclase toxin CyaA is modified by the CyaC acyltransferase at residues K860 and K983, predominantly by the C16:0 chain in *Bordetella pertussis* and by the C16:0 and C16:1 chains in *E. coli* [16,22–26]. We have recently demonstrated that it is the RTX toxin-activating acyltransferase that selects the type of acyl chain of an appropriate length that is covalently linked to the RTX protoxin. Furthermore, the acyltransferase selects whether the first and/or the second conserved lysine residue of the protoxin is acylated, thereby conferring biological activity to the RTX toxin [16].

Although it has been demonstrated that the acylation of RTX toxins is essential for their cytotoxic activities [15,27–29], the molecular mechanisms by which the attached acyl chains confer activity to the RTX toxins remain poorly understood. It has been shown that the acyl chains linked to HlyA are required for the irreversible insertion of the toxin into the target membrane [30] and for the oligomerization of the toxin in membrane microdomains [31]. The acyl chains covalently attached to CyaA have been shown to play an important structural role in the folding of the toxin molecule into a biologically active conformation [32,33] and in the irreversible and productive interaction of CyaA with cells expressing its receptor, the integrin CD11b/CD18 [29,34].

To gain further insights into the acylation of RtxA, we investigated here the importance of the conserved residues K558 and K689 for the interaction of the protoxin proRtxA with the acyltransferase RtxC. Additionally, we examined the significance of acyl chains that selectively modify either the first or the second lysine residue for the binding and cytolytic (pore-forming) activity of RtxA.

2. Materials and methods

2.1. Bacterial strains and growth conditions

E. coli strain XL1-Blue (Stratagene, La Jolla, CA, USA) was used in this work for DNA manipulations and was grown at 37 °C in Luria-Bertani medium supplemented with 150 μg/ml of ampicillin for plasmid-containing strains. *E. coli* strain BL21 (Novagen, Madison, WI, USA) carrying the plasmid pMM100 (encoding LacI and tetracycline resistance) was used for expression of RtxA variants and was grown at 37 °C in MDO medium (yeast extract, 20 g/l; KH_2PO_4, 1 g/l; K_2HPO_4, 3 g/l; glycerol, 20 g/l; Na_2SO_4, 0.5 g/l; NH_4Cl, 2 g/l; thiamine hydrochloride, 0.01 g/l) with 12.5 μg/ml of tetracycline and 150 μg/ml of ampicillin. *E. coli* strain BTH101 (Euromedex, Souffelweyersheim, France) is a non-reverting adenylate cyclase-deficient reporter strain that was used in bacterial adenylate cyclase two-hybrid system assays according to the manufacturer's instructions.

2.2. Plasmids and plasmid construction

The previously constructed plasmids, pT7*rtxC-rtxA* for the expression of RtxC-activated RtxA and pT7*rtxA* for the expression of nonacylated RtxA, were used in this study [15]. Oligonucleotide-directed PCR mutagenesis was used to construct pT7*rtxC-rtxA*-derived plasmids for the expression of RtxC-activated RtxA mutants with single substitutions K558R, K558Q, K689R or K689Q, or with double substitutions K558R+K689R or K558Q+K689Q.

To construct plasmids for the two-hybrid system (Euromedex, Souffelweyersheim, France), the *rtxA* segment encoding residues 529–718 of the protoxin was amplified from pT7*rtxC-rtxA* and fused in frame with a DNA segment encoding the T18 fragment in the plasmid pUT18 for the expression of the proRtxA$_{529-718}$-T18 fusion or in the plasmid pUT18C for the expression of the T18-proRtxA$_{529-718}$ fusion. Similarly, the *rtxA* segments encoding residues 529–623 and 624–718 of the protoxin were amplified from pT7*rtxC-rtxA* and fused in frame with a DNA segment encoding the T18 fragment in pUT18C for the expression of the T18-proRtxA$_{529-623}$ or T18-proRtxA$_{624-718}$ fusion, respectively. Plasmids for the expression of the fusion proteins T18-proRtxA$_{529-718}$, T18-proRtxA$_{529-623}$ and T18-proRtxA$_{624-718}$ with substitutions of the K558 and/or K689 residues were constructed by in frame fusion of mutated *rtxA* segments, amplified from the pT7*rtxC-rtxA*-derived plasmids, with a DNA segment encoding the T18 fragment in pUT18C.

The *rtxC* gene encoding full-length RtxC was amplified from pT7*rtxC-rtxA* and fused in frame with a DNA segment encoding the T25 fragment in pKNT25 for the expression of the RtxC-T25 fusion or in pKT25 for the expression of the T25-RtxC fusion.

2.3. Bacterial adenylate cyclase two-hybrid assay

The bacterial adenylate cyclase two-hybrid (BACTH) system (Euromedex, Souffelweyersheim, France) allows *in vivo* screening of functional interactions between two putative interacting proteins, which are genetically fused to two complementary fragments (T25 and T18) of the enzymatic adenylate cyclase domain of *B. pertussis* CyaA. The association of the two-hybrid proteins results in functional complementation between the T25 and T18 fragments and leads to the production of cAMP, which triggers the transcriptional activation of catabolic operons such as lactose or maltose, thus yielding a characteristic phenotype [35].

The β-galactosidase assay utilizing the BACTH system was performed with bacterial suspensions treated with toluene, according to the protocol provided by the manufacturer. Briefly, plasmids encoding the fusion variants proRtxA$_{529-718}$-T18, T18-proRtxA$_{529-718}$, T18-proRtxA$_{529-623}$, T18-proRtxA$_{624-718}$, or their mutant variants were co-transformed with plasmids encoding the fusion variants RtxC-T25 or T25-RtxC into chemically competent *E. coli* BTH101 cells. Co-transformants of BTH101 were incubated in MacConkey medium agar (Sigma–Aldrich, St. Louis, MO, USA) supplemented with 100 μg/ml of ampicillin, 50 μg/ml of kanamycin, 1 % maltose (final concentration) and 0.5 mM IPTG (isopropyl-D-thiogalactopyranoside) at 30 °C for 48 h. The interaction of the fusion gene products was qualitatively detected by the appearance of red colonies on MacConkey agar plates. Single colonies were selected for further inoculation in 3 ml of Luria-Bertani (LB) liquid medium containing 100 μg/ml ampicillin, 50 μg/ml kanamycin and 0.5 mM IPTG. Cultures were grown at 30 °C and 250 rpm for 16 h until stationary phase was reached. Overnight cultures were diluted 1:5 using M63 minimal medium. Cells were permeabilized by adding 30 μl of toluene and 30 μl of 0.1 % sodium dodecyl sulfate followed by vortexing. The toluene was evaporated from the permeabilized cells by heating at 37 °C for 30 min. Subsequently, 300 μl of the toluene-free permeabilized cell solution was mixed with 700 μl PM2 buffer (70 mM $Na_2HPO_4.12H_2O$, 30 mM $NaH_2PO_4.H_2O$, 30 mM $MgSO_4$, 0.2 mM $MnSO_4$ (pH 7.0) and 100 mM 2-mercaptoethanol). The samples were incubated in a water bath at 28 °C for 5 min.

The enzymatic reaction was initiated by adding 0.25 ml of a 0.4 % ONPG (*o*-nitrophenol-β-galactopyranoside) substrate solution, which was pre-equilibrated at 28 °C. After 1 min, the reaction was stopped by adding 0.5 ml of a 1 M Na_2CO_3 solution. The optical density was measured at 420 nm (OD_{420}) and the values of β-galactosidase activity were calculated according to the following formula: 200 x (OD_{420}/time of incubation (minutes)) x dilution factor. All β-galactosidase assays were performed at least in triplicate and results were adjusted to the OD_{600} of the overnight cultures (1 ml of culture at $OD_{600} = 1$ corresponds to 300 μg dry weight bacteria). β-galactosidase activity was calculated in units (one unit corresponds to 1 nmol of ONPG hydrolyzed per minute at 28 °C) per mg of bacterial cell dry weight. The values were interpreted according to the guidelines provided by the manufacturer. In the absence of interaction, strain BTH101 typically expresses about 100 units/mg of bacterial dry weight. In contrast, when the proteins associate, a range of 700–7000 units/mg is observed depending on the efficiency of the functional complementation. A positive control employing complementation of the leucine zipper of GCN4 (T25-zip/T18-zip) typically yielded values about 6000 units/mg [35].

2.4. Protein production and purification

The RtxA, proRtxA, and RtxA mutants were produced in *E. coli* BL21/pMM100 cells and purified under denaturing conditions to homogeneity by a combination of affinity chromatography on a Ni-NTA agarose column (Qiagen, Germantown, MD, USA) and hydrophobic chromatography on a phenyl-Sepharose CL-4B column (Sigma–Aldrich, St. Louis, MO, USA) as previously described [15].

2.5. Mass spectrometry analysis

Acylation patterns of the RtxA variants modified by the acyltransferase RtxC were determined as previously described [15]. Briefly, the purified RtxA variants were separated by SDS-PAGE, digested in-gel by trypsin (modified sequencing grade, Promega, Madison, WI, USA) and the resulting peptides were analyzed in parallel by liquid chromatography-mass spectrometry (LC-MS, ESI-qTOF (maXis PLUS; Bruker Daltonics, Bremen, Germany)) or off-line peptides separation followed by matrix-assisted laser desorption/ionization time-of-flight (MALDI-TOF (ultraFLEX III; Bruker Daltonics, Bremen, Germany)) MS analysis. Percentage distributions of acyl chains covalently linked to the ε-amino groups of the K558 and K689 residues of the RtxA variants were estimated semi-quantitatively, from the relative intensities of selected ions in reconstructed ion current chromatograms.

2.6. Binding assay

6×10^6 erythrocytes/ml in TNC buffer (50 mM Tris-HCl (pH 7.4), 150 mM NaCl and 2 mM $CaCl_2$) supplemented with 100 mM polyethylene glycol 1500 (TNC-PEG 1500) were incubated with different concentrations (0–8 μg/ml) of the RtxA variants for 15 min at 22 °C. The unbound toxin molecules were washed out with TNC-PEG 1500 or with 100 mM sodium carbonate (pH 10.5) supplemented with PEG 1500, and then with TNC-PEG 1500 supplemented with 1 % fetal calf serum (FCS). The toxin molecules bound to erythrocytes were then labeled for 15 min at 4 °C with a 6x-His Tag monoclonal antibody labeled with Alexa Fluor 488 (Thermo Fisher Scientific, Waltham, MA, USA) and 500x diluted in TNC-PEG 1500 supplemented with 1 % FCS. After washing with TNC-PEG 1500, the cell-bound toxin was determined by flow cytometry using a FACS LSR II instrument (BD Biosciences, San Jose, CA, USA). Data were analyzed using FlowJo software (Tree Star, Ashland, OR, USA) and appropriate gatings were used to exclude cell aggregates and debris. Binding data were deduced from the median fluorescence intensity (MFI) of the bound RtxA variants and expressed as percentage of intact RtxA binding to erythrocytes at a concentration of 8 μg/ml (taken as 100 %).

2.7. Hemoglobin release assay

Sheep erythrocytes (LabMediaServis, Jaromer, Czech Republic) stored in Alsever's Solution (Sigma-Aldrich, St. Louis, MO, USA) were washed with TNC buffer. Washed erythrocytes (5×10^8/ml) were incubated with 200 ng/ml of purified RtxA variants for different times at 37 °C and hemolytic activity was measured by photometric determination (A_{541}) of the hemoglobin release.

2.8. Circular dichroism spectrometry

To determine the effects of the acyl chains and the substitutions of the K558 and K689 residues on the secondary and tertiary structure of RtxA upon its refolding, the circular dichroism spectra of the studied proteins were determined by circular dichroism (CD) spectrometry. The RtxA, proRtxA, RtxA-K558R+K689R and RtxA-K558Q+K689Q proteins were concentrated by ultrafiltration to a final stock concentration of 20 mg/ml using ultrafiltration units with a 10 kDa cutoff membrane (Millipore, Burlington, MA, USA).

For CD in the far ultraviolet wavelength spectrum, the concentrated urea-unfolded RtxA variants were refolded to a concentration of 0.2 mg/ml by rapid dilution in 20 mM Tris-HCl (pH 8.0), 50 mM NaCl, 2 mM $CaCl_2$ buffer. The CD spectra of the proteins were measured in the wavelength range of 200–260 nm using a Suprasil 110-QS quartz cell with 0.1 cm pathlength (Hellma, Müllheim, Germany) and a Chirascan CD spectrometer (Applied Photophysics, Charlotte, NC, USA). Each protein was measured in two independent experiments with three accumulations. The ellipticities (mdeg) were converted to mean residue ellipticities (deg $\times$ cm^2 $\times$ dmol^{-1}).

For the measurement of CD spectra in the near ultraviolet wavelength range of 240–350 nm, the urea-unfolded proteins were refolded by rapid dilution with 50 mM Tris-HCl (pH 8.0), 150 mM NaCl, 2 mM $CaCl_2$ buffer and the CD spectra were measured using a Suprasil 110-HQ quartz cell with 1 cm pathlength (Hellma, Müllheim, Germany). Each protein was measured in two independent experiments with three accumulations.

2.9. Planar lipid bilayers

Overall membrane activities and single-pore conductances and lifetimes of RtxA variants were measured on planar lipid bilayers (black lipid membranes) as previously described [15]. Briefly, measurements were performed in Teflon compartments separated by a diaphragm with a circular hole (diameter 0.5 mm) bearing the membrane, which was formed by the painting method using 3 % soybean lecithin in n-decane–butanol (9:1, vol/vol). Both compartments contained 10 mM Tris-HCl (pH 7.4), 150 mM KCl and 2 mM $CaCl_2$, the temperature was 25 °C. The RtxA variants were prediluted in 50 mM Tris-HCl (pH 8.0), 8 M urea and 2 mM $CaCl_2$ and added to the grounded cis compartment with positive potential. The membrane current was registered by Ag/AgCl electrodes (Theta) with salt bridges (applied voltage, 50 mV), amplified with an LCA-200-10G amplifier (Femto, Berlin, Germany) and digitized with a LabQuest Mini A/D converter (Vernier, Beaverton, OR, USA). For lifetime determination, approximately 150 individual pore openings were recorded and the dwell times were determined using QuB software [36] with a 100 Hz low-pass filter. The kernel density estimation was fitted with an exponential function using Gnuplot software. The relevant model was selected by the $\chi 2$ value.

2.10. Statistical analysis

Statistical significance was calculated by one-way or two-way ANOVA followed by Dunnett's or Sidak's post-test using GraphPad Prism 10.2.2 (GraphPad Software, La Jolla, CA, USA). The results were presented as the arithmetic mean with standard deviation (SD) of the mean. The data generated in this study are available within the article and upon request.

3. Results

3.1. Substitutions of the conserved residue K558, but not K689, partially reduce the interaction between proRtxA and the acyltransferase RtxC in vivo

To investigate the importance of the conserved residues K558 and K689 in the interaction between the protoxin proRtxA and the acyltransferase RtxC, we used a bacterial two-hybrid system that allows *in vivo* screening of functional interactions between two proteins genetically fused to two complementary fragments (T25 and T18) of the catalytic adenylate cyclase domain of *B. pertussis* CyaA [35].

First, we constructed N- and C-terminal fusions of the proRtxA segment, including residues 529–718 (proRtxA$_{529-718}$), with the T18 fragment, and of the full-length RtxC acyltransferase with the T25 fragment (Fig. 1B). Four possible combinations of the fusion proteins were then produced in the *E. coli* strain BTH101 and the efficiency of functional complementation of each fusion protein pair was quantified by measuring enzymatic β-galactosidase activity in bacterial extracts.

As shown in Fig. 2A, all four combinations resulted in functional complementation, with β-galactosidase activities ranging from 53 ± 16 % to 89 ± 11 % of the activity of the leucine zipper control (taken as 100 %), while the background β-galactosidase activity was 11 ± 4 %. The interaction between the T18-proRtxA$_{529-718}$ fusion and the T25-RtxC fusion was almost as strong as the interaction between the leucine zipper (89 ± 11 % and 100 ± 9 %, respectively; Fig. 2A), and this combination of the fusion partners was used in further analyzes.

Next, single or double substitutions of the K558 and K689 residues with arginine (K558R, K689R or K558R+K689R) or glutamine (K558Q, K689Q or K558Q+K689Q) residues, which cannot be covalently modified by acyl chains, were introduced into the T18-proRtxA$_{529-718}$ fusion. The effect of the introduced substitutions on the interaction of the T18-proRtxA$_{529-718}$ mutants with the T25-RtxC fusion was determined as described above. As summarized in Fig. 2B, the single substitutions of the positively charged lysine residues with either the positively charged arginine residues (K558R and K689R) or the neutral glutamine residues (K558Q and

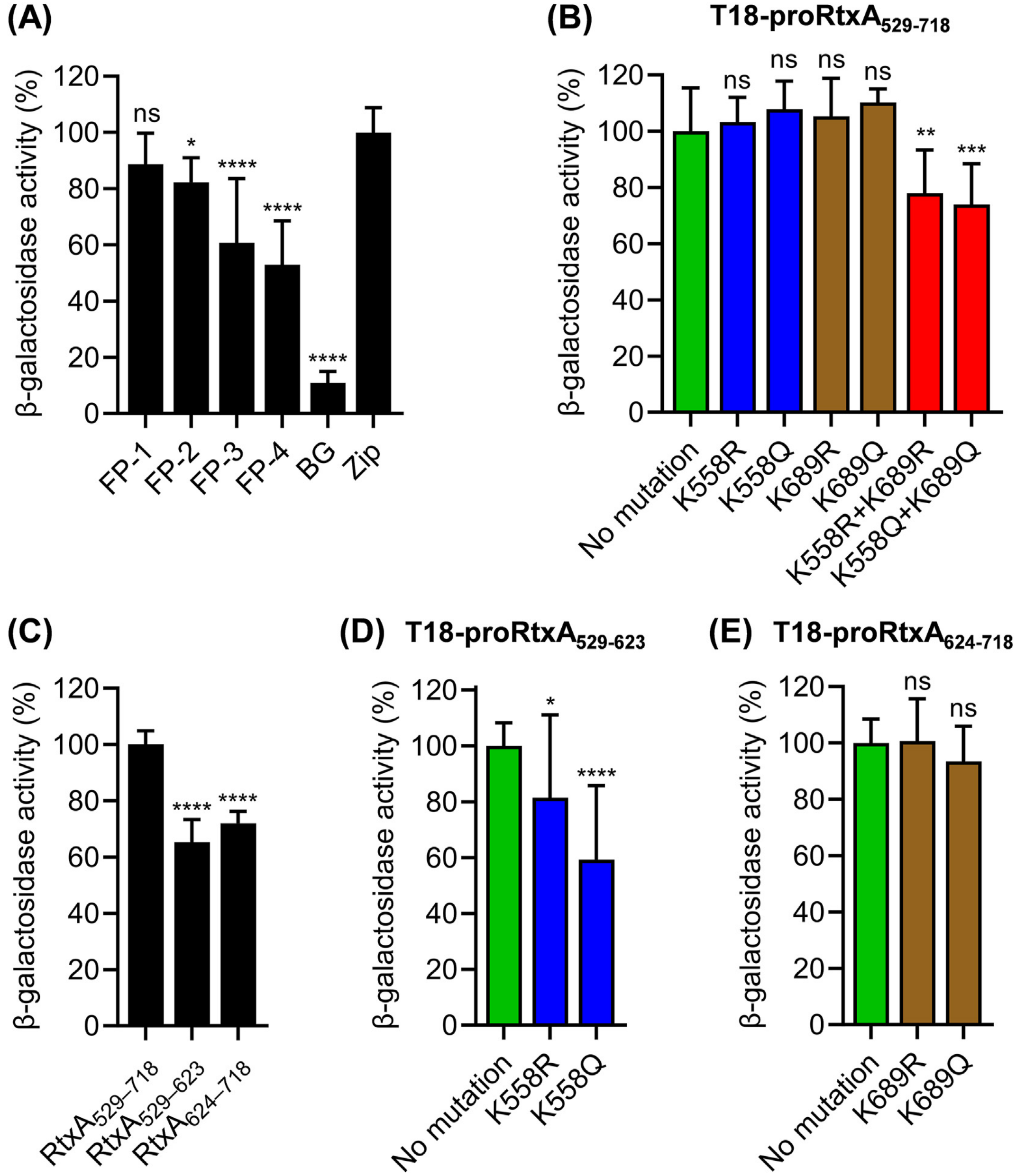

Fig. 2. The conserved residue K558, but not K689, is partially involved in the interaction of proRtxA with the acyltransferase RtxC *in vivo*. (A) The efficiency of functional complementation of four different fusion pairs was quantified by measuring β-galactosidase activity in bacterial extracts of the *E. coli* strain BTH101. The fusion pairs included FP-1 (T18-proRtxA$_{529-718}$ x T25-RtxC), FP-2 (proRtxA$_{529-718}$-T18 x T25-RtxC), FP-3 (T18-proRtxA$_{529-718}$ x RtxC-T25) and FP-4 (proRtxA$_{529-718}$-T18 x RtxC-T25). BG indicates background; Zip, the leucine zipper of GCN4, was used as a positive control for complementation (taken as 100 %). **(B)** The efficiency of functional complementation of the T25-RtxC fusion with the T18-proRtxA$_{529-718}$ fusion variants, which contained the indicated single or double substitutions of the K558 and K689 residues, was quantified as described in (A). **(C)** The efficiency of functional complementation of the T25-RtxC fusion with T18-proRtxA$_{529-623}$, T18-proRtxA$_{624-718}$ or T18-proRtxA$_{529-718}$ (taken as 100 %) was quantified as in (A). The efficiency of functional complementation of the T25-RtxC fusion with the T18-proRtxA$_{529-623}$ **(D)** or T18-proRtxA$_{624-718}$ **(E)** fusion variants containing the indicated single substitutions was quantified as in (A). Each bar represents the mean with SD of three (A, B and C), seven (D) or five (E) independent experiments performed in triplicate (*, $p < 0.05$; **, $p < 0.01$; ***, $p < 0.001$; ****, $p < 0.0001$; ns, not significant).

K689Q) had no significant effect on the interaction of T18-proRtxA$_{529-718}$ with T25-RtxC. In contrast, when the single substitutions were combined within the T18-proRtxA$_{529-718}$ molecule, the interaction was slightly but significantly reduced (to 78 ± 15 % for K558R+K689R and to 74 ± 15 % for K558Q+K689Q) (Fig. 2B).

Finally, we analyzed the effect of the lysine substitutions on the interaction of proRtxA with RtxC for each of the conserved lysine residues separately. For this purpose, the proRtxA$_{529-718}$ fragment of the T18-proRtxA$_{529-718}$ fusion was genetically split into two fragments: proRtxA$_{529-623}$, which contains the K558 residue, and proRtxA$_{624-718}$, which contains the K689 residue (Fig. 1B). As shown in Fig. 2C, both T18-proRtxA$_{529-623}$ and T18-proRtxA$_{624-718}$ interacted with T25-RtxC with a similar efficiency (65 ± 8 % and 72 ± 4 %, respectively), which was lower than the efficiency of the interaction between T18-proRtxA$_{529-718}$ and T25-RtxC (100 ± 5 %). As shown in Fig. 2D, the single substitutions K558R and K558Q partially decreased (to 81 ± 30 % and 59 ± 27 %, respectively) the interaction between T18-proRtxA$_{529-623}$ and T25-RtxC, whereas the single substitutions K689R and K689Q had no significant effect on the interaction of T18-proRtxA$_{624-718}$ with T25-RtxC (Fig. 2E).

These results indicate that substitutions of the conserved residue K558, but not K689, partially reduce the interaction between proRtxA and RtxC, and that the acyltransferase can interact independently with each of the acylated sites *in vivo*.

3.2. Substitutions of the K689 residue in proRtxA result in a significant increase in the acylation of the K558 residue

To analyze how substitutions of the K558 and K689 residues affect the acylation pattern of RtxA, in particular whether substitutions of the K689 residue can increase the acylation of the K558 residue, we replaced K558, K689 or both lysine residues with arginine or glutamine residues. The mutant RtxA variants were produced in the presence of RtxC in *E. coli* cells and purified from urea-solubilized inclusion bodies using a combination of affinity and hydrophobic chromatography (Fig. 3A). To analyze the acylation pattern of the RtxA variants, trypsin digests of the purified proteins were separated by reversed-phase microcapillary high-performance liquid chromatography and analyzed by MS. The relative amounts of acylated peptides for the two acylated sites were then estimated semiquantitatively from the relative intensities of selected ions in reconstructed ion current chromatograms, as previously described [15,16]. As documented in Table 1, a small proportion of the RtxA molecules (24 %) were acylated with the C14:0 (20 %) and C14:0-OH (4 %) chains at the K558 residue, while the remaining toxin molecules (76 %) were nonacylated at this residue. In contrast, almost all RtxA molecules (99 %) were acylated at the K689 residue, predominantly with the C14:0 (72 %) and C14:0-OH (19 %) chains and to a lesser extent (8 %) with the C12:0 and C16:1 chains (Table 1). When the K558 residue was replaced with either the arginine or glutamine residue, the RtxA-K558R and RtxA-K558Q variants were acylated at the K689 residue similarly to the intact RtxA toxin, and, as expected, no acylation was observed at the newly introduced R558 and Q558 residues (Table 1).

Interestingly, when the second conserved lysine residue was replaced, the RtxA-K689R and RtxA-K689Q variants were acylated at the K558 residue with the C14:0 (48 % and 49 %, respectively) and C14:0-OH (18 % and 12 %, respectively) chains with a significantly higher efficiency than the intact RtxA, while only a small proportion of the K558 residues remained nonacylated (34 % and 39 %, respectively) (Table 1). As expected, no acylation was observed at the R689 and Q689 residues of the RtxA-K689R and RtxA-K689Q variants (Table 1). Similarly, no acylation was detected in the RtxA-K558R+K689R and RtxA-K558Q+K689Q variants in which both conserved lysine residues were replaced by the arginine or glutamine residues (Table 1).

These results show that the substitutions of the K558 residue in proRtxA had no effect on the quantitative acylation of the K689 residue by the acyltransferase RtxC. In contrast, the substitutions of the K689 residue resulted in a significant increase in the acylation of the K558 residue. This suggests that RtxC primarily transfers C14 chains from the acyl-acyl carrier protein (ACP) pool of *E. coli* to the ε-amino group of the conserved K689 residue. When this residue is absent due to the substitution K689R or K689Q, the acyltransferase can modify the K558 residue with a significantly higher efficiency.

3.3. The cell binding capacity of the RtxA mutants corresponds to the extent of the acylation at the K558 and/or K689 residues

Using the RtxA variants with substitutions of the K558 and/or K689 residues, we assessed how their acylation patterns affect the interaction of the toxin with the membrane of sheep erythrocytes, which are commonly used as a simple model to analyze the biological activities of RtxA and other RTX toxins [12,15–17]. To analyze binding, erythrocytes were incubated with different concentrations of the purified RtxA variants (0–8 μg/ml) for 15 min. After washing, the cell-bound toxin molecules were stained with a fluorescently labeled anti-hexahistidine monoclonal antibody and detected by flow cytometry. To prevent toxin-mediated lysis of erythrocytes, the entire experiment was performed in the presence of PEG 1500, which served as an osmoprotectant [17].

As shown in Fig. 3B, the RtxA-K558R and RtxA-K558Q variants, which were not acylated at the R/Q558 residue but were fully acylated at the K689 residue (Table 1), demonstrated a partially reduced binding capacity to erythrocytes compared to intact RtxA, on average by 18 % for RtxA-K558R and by 25 % for RtxA-K558Q (calculated from binding values determined at all tested concentrations). As further shown in Fig. 3B, the RtxA-K689R and RtxA-K689Q variants, which were acylated at the K558 residue (66 % and 61 %, respectively), and nonacylated at the R/Q689 residue (Table 1), also exhibited reduced binding capacity to erythrocytes compared to intact RtxA, on average by 54 % for RtxA-K689R and by 71 % for RtxA-K689Q. Furthermore, the mutant variants were irreversibly inserted into the erythrocyte membrane, as they could not be removed with 0.1 M alkaline carbonate buffer (pH 10.5), which is used to remove proteins loosely associated with the membrane. As further shown in Fig. 3B, the two nonacylated mutants, RtxA-K558R+K689R and RtxA-K558Q+K689Q, exhibited negligible binding capacity on erythrocytes, similar to that of the nonacylated proRtxA protoxin.

To investigate whether the acyl chains covalently attached to RtxA play a structural role in the folding of the toxin molecule into a biologically active conformation, as demonstrated for CyaA [32,33], we analyzed RtxA, nonacylated proRtxA and the nonacylated mutants using circular dichroism (CD) spectroscopy. When the urea-denatured RtxA proteins were refolded in the presence of a physiological concentration of calcium ions (2 mM), the far- and near-UV CD spectra indicated that the nonacylated RtxA variants refolded differently from the acylated RtxA toxin (Fig. 3C).

All these results indicate that the acyl chains of RtxA enable the irreversible insertion of the toxin into the erythrocyte membrane, the efficiency of which corresponds to the extent of the acylation at the K558 and K689 residues (cf. Fig. 3B and Table 1). In contrast, the nonacylated RtxA variants showed only residual binding to erythrocytes and their final structure differed from that of the acylated RtxA, suggesting that the acyl chains may be involved in the folding of the toxin molecule.

3.4. All RtxA mutants exhibit low hemolytic activity, but their pore characteristics are similar to those of intact RtxA

To determine hemolytic activity of the RtxA variants, erythrocytes were incubated with 200 ng/ml of the purified toxin variants for various times and hemolytic activity was measured as the amount of released hemoglobin by photometric determination. As documented in Fig. 4A, intact RtxA lysed 56 ± 13 % of erythrocytes within 10 min of incubation and almost complete lysis (87 ± 7 %) was observed when erythrocytes were incubated with the toxin for 1 h. Interestingly, only residual lysis was observed over the 60-min testing period when erythrocytes were incubated with RtxA-K558R or RtxA-K558Q (Fig. 4A), which lacked acylation at the K558 residue but were fully acylated at the K689 residue, similar to intact RtxA (Table 1). Similarly, only residual lysis was observed when erythrocytes were incubated with RtxA-K689R or RtxA-K689Q (Fig. 4A), which lacked acylation at the K689 residue but were substantially acylated at the K558 residue (>60 %), it means more than intact RtxA (Table 1). As expected, the doubly substituted and nonacylated variants, RtxA-K558R+K689R and RtxA-K558Q+K689Q, lysed erythrocytes with very low efficiency,

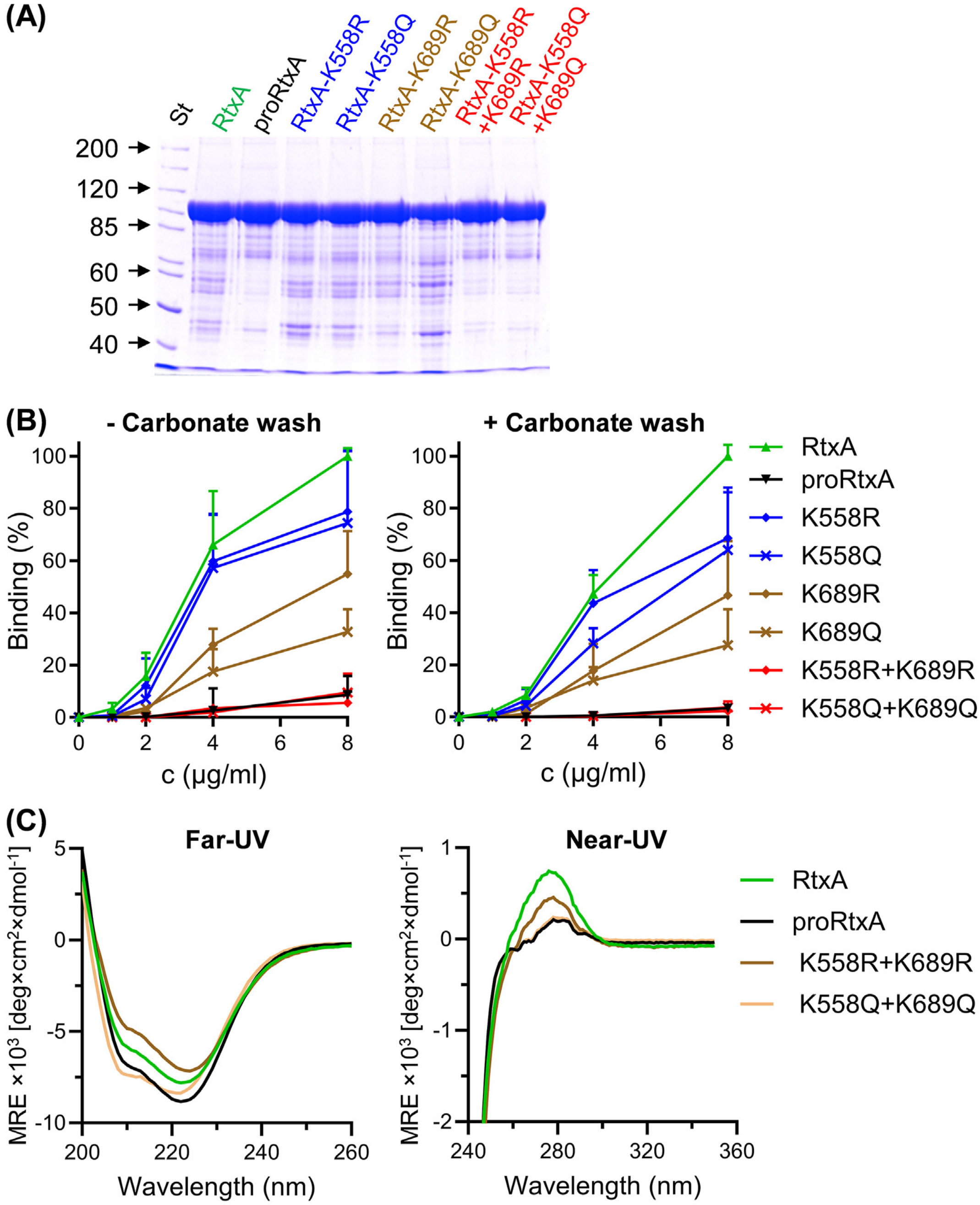

Fig. 3. The cell binding capacity of the RtxA mutants corresponds to the extent of their acylation at the conserved residues K558 and/or K689. (A) A set of pT7*rtxC-rtxA*-derived plasmids was used to produce the RtxA variants in *E. coli* BL21/pMM100 cells. The RtxA variants were purified from urea-solubilized inclusion bodies using a combination of affinity chromatography on Ni-NTA agarose and hydrophobic chromatography on phenyl-Sepharose. Samples were analyzed on a 7.5 % polyacrylamide gel and stained with Coomassie Blue. St, Molecular mass standards. **(B)** Sheep erythrocytes (6×10^6/ml) were incubated with different concentrations of the purified RtxA variants in the presence of an osmoprotectant (PEG 1500) for 15 min at 22 °C. After washing, without or with alkaline carbonate, the cell-bound toxin molecules were detected with a fluorescently labeled anti-hexahistidine monoclonal antibody by flow cytometry. Binding data were calculated from the MFI values and expressed as percentage of the intact RtxA binding to erythrocytes at a concentration of 8 μg/ml (taken as 100 %). Each point represents the mean with SD of at least five independent experiments performed in duplicate with two different toxin preparations. The SD values were below 3, 11, 21 and 28 % at concentrations of 1, 2, 4 and 8 μg/ml, respectively. The binding of proRtxA and the RtxA mutants (except for RtxA-K558R and RtxA-K558Q in the left panel and RtxA-K558R in the right panel) to erythrocytes was significantly lower than that of intact RtxA ($p < 0.0001$ at concentrations of 4 and 8 μg/ml). **(C)** Far-UV and near-UV CD spectra of the indicated RtxA variants measured in the presence of 2 mM $CaCl_2$. The data correspond to the average of two independent experiments with three accumulations per spectrum. MRE, mean residue ellipticity.

similar to the nonacylated proRtxA protoxin produced in the absence of RtxC (Fig. 4A). These results indicate that the complete acylation of the single K689 residue of the RtxA-K558R or RtxA-K558Q variants by the C14 acyl chains (Table 1) was insufficient for the hemolytic activity or that this activity was almost completely abolished by the introduced K558R and K558Q substitutions. Similar conclusions can be drawn from the results obtained with the RtxA-K689R or RtxA-K689Q variants, which were more efficiently acylated at the single K558 residue (>60 %) than intact RtxA (24 %; Table 1).

To determine whether the residual hemolytic (pore-forming) activity of the RtxA mutants on erythrocytes was caused by the low

Table 1
Acylation status of the RtxA variants modified by the RtxC acyltransferase.

Residue[a]	Acyl chain[a]	Relative distribution of acyl chains in intact RtxA (WT) and its variants (%)[b]						
		WT	K558R	K558Q	K689R	K689Q	K558R+K689R	K558Q+K689Q
558	None	76	100	100	34	39	100	100
	C14:0	20	0	0	48	49	0	0
	C14:0-OH	4	0	0	18	12	0	0
689	None	1	1	1	100	100	100	100
	C12:0	1	0	1	0	0	0	0
	C14:0	72	72	70	0	0	0	0
	C14:0-OH	19	17	17	0	0	0	0
	C16:1	7	10	11	0	0	0	0

[a] The RtxA variants were produced in the presence of the RtxC acyltransferase in *E. coli* BL21/pMM100 cells, purified close to homogeneity and analyzed by MS. The ε-amino group of the K558 and K689 residues were found to be modified by lauroyl (C12:0), myristoyl (C14:0), hydroxymyristoyl (C14:0-OH) and/or palmitoleyl (C16:1) chains.

[b] The percentage distributions of acyl chains covalently linked to the ε-amino group of the K558 and K689 residues of RtxA were semiquantitatively estimated from the relative intensities of selected ions in reconstructed ion current chromatograms. The average values were calculated from determinations performed with two different toxin preparations in triplicate.

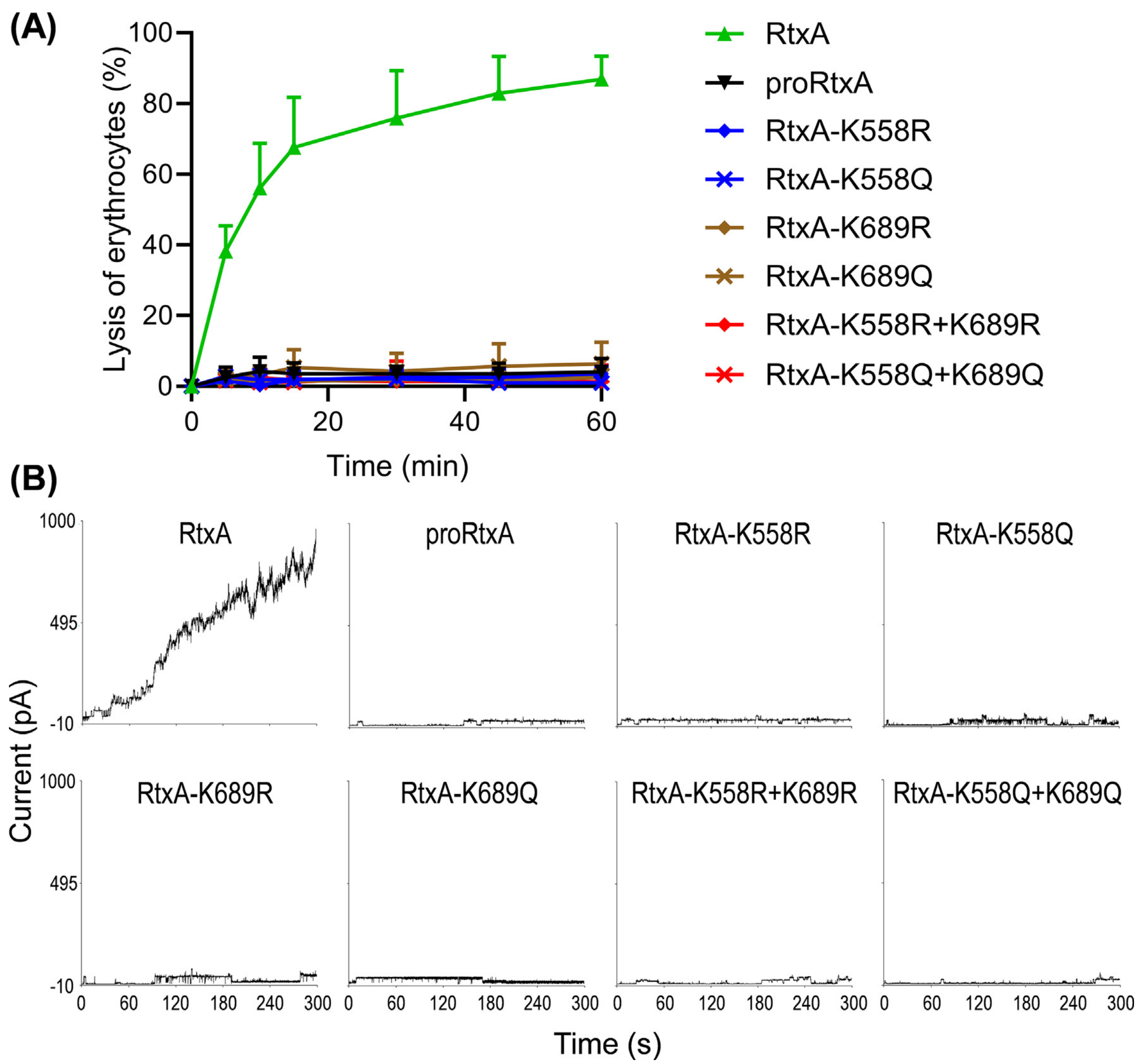

Fig. 4. All RtxA mutants exhibit negligible hemolytic activity in erythrocytes and correspondingly low overall membrane activity in planar lipid membranes. (A) Sheep erythrocytes (5×10^8/ml) were incubated with 200 ng/ml of the purified RtxA variants at 37 °C. The lysis of erythrocytes was measured as the amount of released hemoglobin by photometric determination (A_{541}) at the indicated time points. Each point is expressed as percentage of complete erythrocyte lysis (taken as 100 %) and represents the mean with SD of three independent experiments performed in duplicate with two different toxin preparations. All RtxA variants lysed erythrocytes with significantly lower efficiency than intact RtxA ($p < 0.0001$ at all tested time points >0). No statistically significant differences in erythrocyte lysis were observed between proRtxA and the RtxA variants, nor among the RtxA variants themselves ($p > 0.05$). **(B)** Overall membrane activities of the RtxA variants on asolectin membranes in the presence of 250 pM purified proteins. The aqueous phase contained 10 mM Tris-HCl (pH 7.4), 150 mM KCl and 2 mM $CaCl_2$. The temperature was maintained at 25 °C, the applied voltage was 50 mV and the recording was filtered at 10 Hz.

propensity of the toxin variants to form membrane pores or by different properties of the individual pores, we analyzed the overall membrane activity as well as single-pore conductance and lifetime of the pores formed by the toxin variants in artificial planar lipid bilayers made of 3 % asolectin. As shown in Fig. 4B, all RtxA mutants exhibited very low overall membrane activity on artificial lipid bilayers compared to that of intact RtxA. However, as calculated from single-pore recordings and shown in Fig. 5A, the most frequent conductance values of the pores formed by the RtxA mutants ranged from 373 ± 69 pS to 448 ± 77 pS and were comparable to the conductance of the pores formed by intact RtxA (434 ± 53 pS). Furthermore, the overall membrane activities and conductance values of all RtxA mutants were similar to those of the nonacylated proRtxA protoxin (Figs. 4B and 5A). As shown in Fig. 5B, despite the natural heterogeneity in single-pore lifetimes caused by pore formation dynamics, two major opposing trends were observed in the most frequent lifetime values of the RtxA mutants. While RtxA-K558Q and RtxA-K689Q exhibited slightly higher most frequent lifetime values (2456 ± 138 ms and 2599 ± 165 ms, respectively), RtxA-K558R, RtxA-K689R and RtxA-K558R+K689R displayed slightly lower values (1417 ± 137 ms, 1477 ± 94 ms and 1251 ± 102, respectively) compared to the lifetime value of intact RtxA (1657 ± 110 ms). Finally, the most frequent lifetime values of RtxA-K558Q+K689Q and proRtxA (1671 ± 121 ms and 1589 ± 123 ms, respectively) were comparable to the lifetime value of intact RtxA (1657 ± 110 ms). All these results indicate that the differences in the acylation pattern and/or the introduced substitutions of the conserved lysine residues strongly reduced the propensity of the RtxA mutants to form functional pores in the lipid bilayer, while having no or minimal impact on the overall properties of the individual pores.

4. Discussion

To gain deeper insights into the acylation of RtxA, we investigated here whether the two conserved lysine residues, K558 and K689, are involved in the interaction of the proRtxA protoxin with the RtxC acyltransferase and how differently acylated variants of RtxA interact with target membranes and form membrane pores.

To investigate the importance of the K558 and K689 residues for the interaction of proRtxA with RtxC, we used the bacterial two-hybrid system, which has been successfully used to test the ability of the ApxIC acyltransferase and its mutant variants to dimerize or interact with ACP or an HlyA protoxin fragment [37]. As a first step, we tested which of the fusion pairs, including the pro-$RtxA_{529-718}$ segment fused to the N- or C-terminus of T18 and RtxC fused to the N- or C-terminus of T25, allows functional complementation. Our results showed that all four tested combinations led to functional complementation *in vivo*, albeit with varying efficiencies. The strongest interaction was observed with the T18-$proRtxA_{529-718}$ x T25-RtxC fusion pair, while the weakest interaction was obtained with the $proRtxA_{529-718}$-T18 x RtxC-T25 fusion pair, showing a difference of 36 % between these two fusion pairs. This demonstrates that the fusion of $proRtxA_{529-718}$ and RtxC to the C-terminus of T18 and T25, respectively, is more favorable for functional complementation than the N-terminal fusion, likely due to lower steric hindrance between the interacting proteins. To achieve optimal results in functional complementation, it is therefore important to analyze to which end of the T18 and T25 fragments the tested interacting proteins are fused.

Our data further showed that RtxC interacts independently with each of the acylated sites of proRtxA *in vivo*. Nevertheless, the interaction of T25-RtxC with the T18-$proRtxA_{529-623}$ or T18-$proRtxA_{624-718}$ fusion, in which each proRtxA fragment contains only one of the two conserved acylated sites, was weaker by 35 % and 28 %, respectively, than that of T25-RtxC with the T18-$proRtxA_{529-718}$ fusion, which contains both conserved acylated sites. This suggests that each of the two acylated sites within pro-$RtxA_{529-718}$ may simultaneously interact with a separate T25-RtxC molecule, thus increasing the final signal in the β-galactosidase assay. It also shows that the independent interaction of RtxC with each of the acylated sites of proRtxA *in vivo* depends only on 95 amino acid residues. Previously, an independent interaction between the HlyC acyltransferase and the first or second acylated site of proHlyA was reported [38]. Each of the acylated sites required 15–30 residues for basal HlyC recognition and 50–80 residues for wild-type acylation at the K564 and K690 residues.

Next, we showed that single substitutions of the K558 and K689 residues by positively charged arginine or uncharged glutamine residues had no significant effect on the interaction between T18-$proRtxA_{529-718}$ and T25-RtxC. Only a weak decrease in interaction was observed when the double substitutions K558R+K689R (by 22 %) and K558Q+K689Q (by 26 %) were introduced into the T18-$proRtxA_{529-718}$ fusion. Further analysis of each of the conserved acylated sites separately showed that the single substitutions K558R and K558Q partially decrease the interaction of RtxC with the first acylated site, whereas the interaction of RtxC with the second acylated site was not affected by the introduced K689R and K689Q substitutions. This indicates that the substitutions of the conserved residue K558, but not K689, partially reduce the interaction of the protoxin with the acyltransferase RtxC *in vivo*.

We previously showed that recombinant HlyC-modified HlyA, CyaC-modified CyaA and RtxC-modified RtxA produced in the same *E. coli* strain were completely acylated at the second conserved lysine residue. While HlyA and CyaA were also considerably acylated at the first conserved lysine residue (90 % in HlyA and 69 % in CyaA), acylation of the first lysine residue of RtxA (K558) was detected only in a small proportion of toxin molecules (2–23 %), depending on the toxin batch [15,16]. Here, we analyzed whether single substitutions of the K689 residue of proRtxA by an arginine or glutamine residue, which cannot be covalently modified by acyl chains, can increase the acylation of the K558 residue. As demonstrated by MS, the K689R and K689Q substitutions introduced into proRtxA indeed substantially increased (on average by 40 %) the acylation of the K558 residue compared to the intact toxin. As expected, the K558R and K558Q substitutions introduced into the first acylated site of proRtxA had no effect on the complete acylation of the K689 residue. These results show that RtxC preferentially transfers acyl chains from the acyl-ACP pool of *E. coli* to the ε-amino group of the conserved K689 residue of proRtxA. However, when this residue is absent due to the K689R or K689Q substitution, the acyltransferase modifies the K558 residue with a substantially higher efficiency.

Our binding experiments showed that intact RtxA and monoacylated RtxA mutants are inserted into the membrane of sheep erythrocytes, which are commonly used as a simple model for testing the biological activities of RtxA and other RTX toxins [12,15–17]. The intact RtxA toxin, which was acylated at K558 and K689 in 24 % and 99 % of the molecules, respectively, exhibited the highest binding capacity. The RtxA-K558R and RtxA-K558Q variants, which were not acylated at the R/Q558 residue but were completely acylated at the K689 residue, showed a proportionally lower binding capacity to erythrocytes (on average by 22 %) compared to intact RtxA. Similarly, the RtxA-K689R and RtxA-K689Q variants, which were acylated at the K558 residue in 66 % and 61 % of the molecules, respectively, and nonacylated at the R/Q689 residue, also exhibited a proportionally lower binding capacity to erythrocytes (on average by 54 % for RtxA-K689R and by 71 % for RtxA-K689Q) compared to intact RtxA. In addition, both the intact RtxA toxin and the monoacylated RtxA variants were

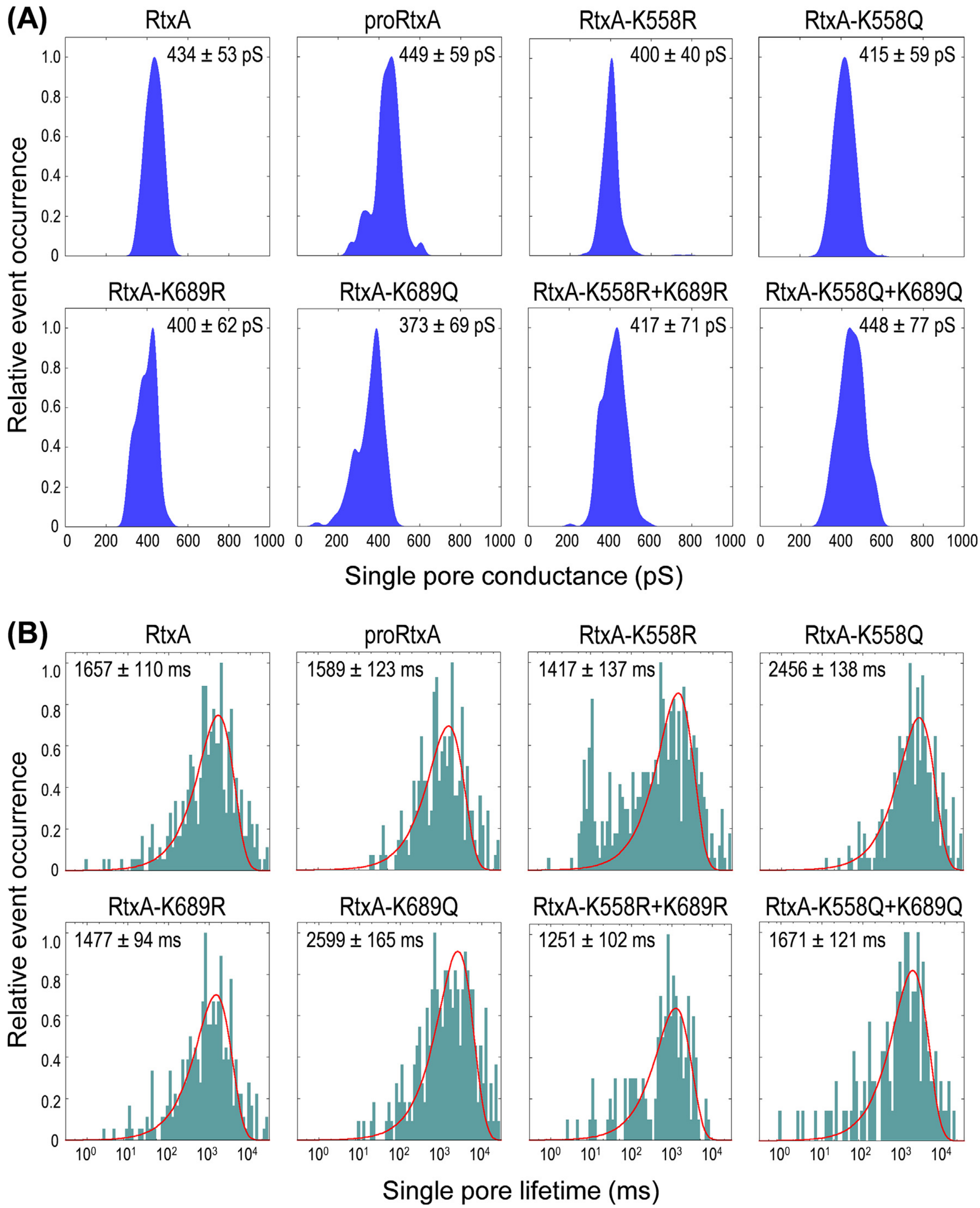

Fig. 5. The RtxA mutants form pores with similar single-pore conductance and lifetime as intact RtxA. (A) Kernel density estimation of single-pore conductances calculated from single-pore recordings (>400 events) acquired on several different asolectin membranes with 10 pM RtxA or its mutant variants under the same conditions as described in Fig. 4B. The numbers represent the most frequent conductance values ± standard deviations of the pores formed by the RtxA variants. **(B)** To determine lifetimes, approximately 150 individual pore openings were recorded on several different asolectin membranes with 10 pM RtxA or its variants under the same conditions as in Fig. 5. The logarithmic histogram of dwell times was fitted with an exponential function. The error estimates of the lifetimes were determined by bootstrap analysis. The numbers in each panel represent the most frequent lifetime value ± SD.

irreversibly inserted into the erythrocyte membrane, as they could not be removed with alkaline carbonate buffer. As expected, the RtxA-K558R+K689R and RtxA-K558Q+K689Q variants, which are both nonacylated, exhibited only a very low binding capacity to erythrocytes (on average 6 %), similar to that of the nonacylated proRtxA protoxin. Furthermore, the far- and near-UV CD spectra indicated that all three nonacylated RtxA variants might differ in structure from the acylated RtxA. This observation is consistent with findings of O'Brien and colleagues, who demonstrated that refolded acylated CyaA is more compact and stable than non-acylated proCyaA, due to local and distal acylation-dependent interactions within the toxin. The acyl chains covalently linked to the residues K860 and K983 of CyaA favored a hydrophobic collapse within the apolar segment comprising residues 660–710, which served as a nucleus for the folding of the hydrophobic domain and the acylated region into the native state [33]. Thus, our results showed that the acyl chains of RtxA enable the irreversible insertion of the toxin into the erythrocyte membrane and that the efficiency of toxin binding is in good agreement with the extent of the acylation at the conserved K558 and K689 residues. In contrast, the nonacylated RtxA variants showed only negligible insertion into the erythrocyte membrane due to the absence of the acyl chains, which are most likely also involved in the folding of the RtxA molecule, as previously shown for CyaA [33].

Despite the sufficiently high cell binding capacity, the monoacylated RtxA-K558R/Q and RtxA-K689R/Q variants exhibited only residual hemolytic activity on erythrocytes (less than 7 %). In agreement with this, the monoacylated RtxA variants demonstrated very low overall membrane activity in planar lipid bilayers. However, once a few individual pores were formed by these monoacylated variants, their characteristics, such as single-pore conductance and lifetime, were similar to those of intact RtxA. Thus, despite the irreversible insertion into the membrane, the monoacylated RtxA variants were severely impaired in their ability to form functional pores. This suggests that the hemolytic (pore-forming) activity of the monoacylated RtxA variants with substitutions at either of the two conserved lysine residues was greatly reduced due to the acylation at only one conserved lysine residue or the introduced single substitutions. Since we have shown that biologically active recombinant RtxA is completely acylated at the K689 residue but only partially at the K558 residue (from 2 to 23 %) [15,16], it is more likely that the hemolytic activity of the monoacylated RtxA-K558R and RtxA-K558Q variants was strongly reduced due to the introduced substitutions and not due to the acylation solely at the K689 residue. This conclusion is further supported by our previous observation showing that HlyC-acylated RtxA, which had only a residual acylation at K558 (3 %) and was fully acylated at K689, exhibited the same hemolytic activity as RtxC-acylated RtxA [16].

Observations indicating that substitutions of the two conserved lysine residues, rather than acylation at only one of them, leads to impaired biological activities have also been reported for HlyA and CyaA. Indeed, a significant decrease in hemolytic activity was previously observed for HlyA variants containing single substitutions of the conserved residues K563 (corresponding to K558 of RtxA) and K689 (corresponding to K689 of RtxA) [39]. The HlyA-K563C and HlyA-K689R variants lysed 21 % and 11 % of erythrocytes, respectively, while the HlyA-K563T, HlyA-K689E and HlyA-K689C variants exhibited no hemolytic activity. Similarly, no hemolytic activity was detected with the HlyA-K564R, HlyA-K564L, HlyA-K690R and HlyA-K690L variants (the numbering is shifted by +1 due to a different isoform of HlyA), which were monoacylated both *in vivo* and *in vitro*, as demonstrated by another group [28]. Additionally, negligible or no hemolytic activity was observed with HlyA variants containing single substitutions K564I, K564 M, K690R, K690I or K690 M, as reported in another study [40]. In these three studies, however, it was not determined whether the HlyA mutants were inserted into the erythrocyte membrane. Subsequent research showed that HlyA molecules acylated by mutated HlyC, which contained mostly a mixture of monoacylated HlyA with nonacylated proHlyA, and only small amounts of doubly acylated HlyA, still exhibited significant hemolytic activities, ranging from 27 to 60 % of the activity of the doubly acylated toxin [41]. Additionally, we previously showed that CyaC- and RtxC-acylated HlyA molecules, in which the first conserved lysine residue was only partially acylated (7 % and 27 %, respectively) and the second conserved lysine residue was fully acylated, lysed erythrocytes with the same efficiency as the doubly HlyC-acylated HlyA toxin [16]. Thus, all these observations demonstrate that the monoacylated HlyA variants without introduced substitutions at the conserved lysine residues were as hemolytic as the doubly acylated toxin, or their hemolytic activity was only partially reduced. In contrast, the hemolytic activity of the monoacylated HlyA variants with introduced substitutions at either of the two conserved lysine residues was strongly reduced or completely abolished. This indicates that the single substitutions of the two conserved lysine residues introduced into HlyA can cause such structural effects in the toxin molecule that severely impair hemolytic activity, as observed in this study with RtxA.

When single substitutions of the conserved lysine residues (K860R, K860L, K860C and K983R) were introduced into CyaC-modified recombinant CyaA, the binding of the monoacylated toxin variants to erythrocytes was substantially reduced (to 15–23 % of that of intact CyaA) [24,29]. In contrast to the results obtained here with the corresponding monoacylated RtxA variants, the decrease in the binding capacity of the CyaA variants to erythrocytes was not proportional to the extent of their acylation but was significantly lower. Consistent with the reduced binding capacity, the monoacylated CyaA variants were also substantially impaired in both the translocation of the enzymatic domain across the erythrocyte membrane (1–12 % of that of intact CyaA) and hemolytic activity (3–8 % of that of intact CyaA). Since a previous study indicated that some *Bordetella* strains can produce biologically active CyaA acylated solely at the K983 residue [22], it was concluded that the K860 residue *per se* plays a crucial structural role in the biological activities of CyaA on erythrocytes, regardless of its acylation status [24]. In a subsequent study, CyaA selectively monoacylated at the K983 residue by mutated CyaC was shown to exhibit biological activities on erythrocytes that were proportional to the extent of its acylation at the K983 residue, providing further indication that the acylation of K983 is sufficient for toxin activity [26]. Taken together, the data reported for RtxA, HlyA and CyaA indicate that the acyl linked to the first lysine residue is dispensable for the biological activities of the RTX toxins on erythrocytes and that the first lysine residue cannot be functionally replaced by another amino acid residue. Indeed, even a conservative substitution of the first lysine residue with an arginine residue resulted in a substantial decrease in the biological activities of the RTX toxins, highlighting the irreplaceable structural role of this residue in cytotoxicity [16,24,26,28,29,39–41].

CRediT authorship contribution statement

Humaira Khaliq: Visualization, Validation, Methodology, Investigation, Formal analysis. **Adriana Osickova:** Validation, Supervision, Methodology, Investigation. **Michaela Lichvarova:** Validation, Methodology, Investigation, Formal analysis. **Miroslav Sulc:** Validation, Methodology, Investigation, Formal analysis, Data curation. **Kevin Munoz Navarrete:** Validation, Methodology, Investigation, Formal analysis. **Carlos Espinosa-Vinals:** Visualization, Validation, Methodology, Investigation, Formal analysis. **Jiri Masin:** Writing – review & editing, Methodology, Investigation. **Radim Osicka:** Writing – review & editing, Writing – original draft, Visualization, Validation, Supervision, Methodology, Investigation, Funding acquisition, Formal analysis, Conceptualization.

Funding

This work was supported by project 22-15825S from the Czech Science Foundation (GACR) and by project LM2023053 (Czech National Node to the European Infrastructure for Translational Medicine) from Ministry of Education, Youth and Sports of the Czech Republic. We also acknowledge support from Talking microbes - understanding microbial interactions within One Health framework (CZ.02.01.01/00/22_008/0004597).

Declaration of competing interest

The authors declare that they have no known competing financial interests or personal relationships that could have appeared to influence the work reported in this paper.

Acknowledgements

We would like to thank Sona Kozubova for her excellent technical assistance. Humaira Khaliq and Carlos Espinosa-Vinals are doctoral students at the University of Chemistry and Technology in Prague.

References

[1] K. Moumile, J. Merckx, C. Glorion, P. Berche, A. Ferroni, Osteoarticular infections caused by *Kingella kingae* in children: contribution of polymerase chain reaction to the microbiologic diagnosis, Pediatr. Infect. Dis. J. 22 (2003) 837–839.
[2] A. Gene, J.J. Garcia-Garcia, P. Sala, M. Sierra, R. Huguet, Enhanced culture detection of *Kingella kingae*, a pathogen of increasing clinical importance in pediatrics, Pediatr. Infect. Dis. J. 23 (2004) 886–888.
[3] I. Verdier, A. Gayet-Ageron, C. Ploton, P. Taylor, Y. Benito, A.M. Freydiere, F. Chotel, J. Berard, P. Vanhems, F. Vandenesch, Contribution of a broad range polymerase chain reaction to the diagnosis of osteoarticular infections caused by *Kingella kingae*: description of twenty-four recent pediatric diagnoses, Pediatr. Infect. Dis. J. 24 (2005) 692–696.
[4] G. Dubnov-Raz, M. Ephros, B.Z. Garty, Y. Schlesinger, A. Maayan-Metzger, J. Hasson, I. Kassis, O. Schwartz-Harari, P. Yagupsky, Invasive pediatric *Kingella kingae* Infections: a nationwide collaborative study, Pediatr. Infect. Dis. J. 29 (2010) 639–643.
[5] P. Yagupsky, E. Porsch, J.W. St Geme, 3rd, *Kingella kingae*: an emerging pathogen in young children, Pediatrics 127 (2011) 557–565.
[6] D. Ceroni, V. Dubois-Ferrière, A. Cherkaoui, L. Lamah, G. Renzi, P. Lascombes, B. Wilson, J. Schrenzel, 30 years of study of *Kingella kingae*: post tenebras, lux, Future Microbiol. 8 (2013) 233–245.
[7] N. Principi, S. Esposito, *Kingella kingae* infections in children, BMC Infect. Dis. 15 (2015) 260.
[8] P. Yagupsky, *Kingella kingae*: carriage, transmission, and disease, Clin. Microbiol. Rev. 28 (2015) 54–79.
[9] C. Gouveia, M. Duarte, S. Norte, J. Arcangelo, M. Pinto, C. Correia, M.J. Simoes, H. Canhao, D. Tavares, *Kingella kingae* displaced *S. aureus* as the most common cause of acute septic arthritis in children of all ages, Pediatr. Infect. Dis. J. 40 (2021) 623–627.
[10] I. Linhartova, L. Bumba, J. Masin, M. Basler, R. Osicka, J. Kamanova, K. Prochazkova, I. Adkins, J. Hejnova-Holubova, L. Sadilkova, J. Morova, P. Sebo, RTX proteins: a highly diverse family secreted by a common mechanism, FEMS Microbiol. Rev. 34 (2010) 1076–1112.
[11] I. Linhartova, R. Osicka, L. Bumba, J. Masin, P. Sebo, RTX Toxins: a Review, Microbial Toxins, Toxinology ed., Springer, Dordrecht, the Netherlands, 2015.
[12] K. Filipi, W.U. Rahman, A. Osickova, R. Osicka, *Kingella kingae* RtxA cytotoxin in the context of other RTX toxins, Microorganisms 10 (2022) 518.
[13] T.E. Kehl-Fie, J.W. St Geme 3rd, Identification and characterization of an RTX toxin in the emerging pathogen *Kingella kingae*, J. Bacteriol. 189 (2007) 430–436.
[14] D.W. Chang, Y.A. Nudell, J. Lau, E. Zakharian, N.V. Balashova, RTX toxin plays a key role in *Kingella kingae* virulence in an infant rat model, Infect. Immun. 82 (2014) 2318–2328.
[15] A. Osickova, N. Balashova, J. Masin, M. Sulc, J. Roderova, T. Wald, A.C. Brown, E. Koufos, E.H. Chang, A. Giannakakis, E.T. Lally, R. Osicka, Cytotoxic activity of *Kingella kingae* RtxA toxin depends on post-translational acylation of lysine residues and cholesterol binding, Emerg. Microb. Infect. 7 (2018) 178.
[16] A. Osickova, H. Khaliq, J. Masin, D. Jurnecka, A. Sukova, R. Fiser, J. Holubova, O. Stanek, P. Sebo, R. Osicka, Acyltransferase-mediated selection of the length of the fatty acyl chain and of the acylation site governs activation of bacterial RTX toxins, J. Biol. Chem. 295 (2020) 9268–9280.
[17] E. Ruzickova, M. Lichvarova, A. Osickova, K. Filipi, D. Jurnecka, H. Khaliq, C. Espinosa-Vinals, P. Pompach, J. Masin, R. Osicka, Two pairs of back-to-back alpha-helices of *Kingella kingae* RtxA toxin are crucial for the formation of a membrane pore, Int. J. Biol. Macromol. 283 (2024) 137604.
[18] W.U. Rahman, A. Osickova, N. Klimova, J. Lora, N. Balashova, R. Osicka, Binding of *Kingella kingae* RtxA toxin depends on cell surface oligosaccharides, but not on β_2 integrins, Int. J. Mol. Sci. 21 (2020) 9092.
[19] W.U. Rahman, R. Fiser, R. Osicka, *Kingella kingae* RtxA toxin interacts with sialylated gangliosides, Microb. Pathog. 181 (2023) 106200.
[20] I. Bárcena-Uribarri, R. Benz, M. Winterhalter, E. Zakharian, N. Balashova, Pore forming activity of the potent RTX-toxin produced by pediatric pathogen *Kingella kingae*: characterization and comparison to other RTX-family members, Biochim. Biophys. Acta 1848 (2015) 1536–1544.
[21] K.B. Lim, C.R. Walker, L. Guo, S. Pellett, J. Shabanowitz, D.F. Hunt, E.L. Hewlett, A. Ludwig, W. Goebel, R.A. Welch, M. Hackett, *Escherichia coli* alpha-hemolysin (HlyA) is heterogeneously acylated in vivo with 14-, 15-, and 17-carbon fatty acids, J. Biol. Chem. 275 (2000) 36698–36702.
[22] M. Hackett, L. Guo, J. Shabanowitz, D.F. Hunt, E.L. Hewlett, Internal lysine palmitoylation in adenylate cyclase toxin from *Bordetella pertussis*, Science 266 (1994) 433–435.
[23] M. Hackett, C.B. Walker, L. Guo, M.C. Gray, S. Van Cuyk, A. Ullmann, J. Shabanowitz, D.F. Hunt, E.L. Hewlett, P. Sebo, Hemolytic, but not cell-invasive activity, of adenylate cyclase toxin is selectively affected by differential fatty-acylation in *Escherichia coli*, J. Biol. Chem. 270 (1995) 20250–20253.
[24] T. Basar, V. Havlicek, S. Bezouskova, P. Halada, M. Hackett, P. Sebo, The conserved lysine 860 in the additional fatty-acylation site of *Bordetella pertussis* adenylate cyclase is crucial for toxin function independently of its acylation status, J. Biol. Chem. 274 (1999) 10777–10783.
[25] V. Havlicek, L. Higgins, W. Chen, P. Halada, P. Sebo, H. Sakamoto, M. Hackett, Mass spectrometric analysis of recombinant adenylate cyclase toxin from *Bordetella pertussis* strain 18323/pHSP9, J. Mass Spectrom. 36 (2001) 384–391.
[26] T. Basar, V. Havlicek, S. Bezouskova, M. Hackett, P. Sebo, Acylation of lysine 983 is sufficient for toxin activity of *Bordetella pertussis* adenylate cyclase. Substitutions of alanine 140 modulate acylation site selectivity of the toxin acyltransferase CyaC, J. Biol. Chem. 276 (2001) 348–354.
[27] E.M. Barry, A.A. Weiss, I.E. Ehrmann, M.C. Gray, E.L. Hewlett, M.S. Goodwin, *Bordetella pertussis* adenylate cyclase toxin and hemolytic activities require a second gene, *cyaC*, for activation, J. Bacteriol. 173 (1991) 720–726.
[28] P. Stanley, L.C. Packman, V. Koronakis, C. Hughes, Fatty acylation of two internal lysine residues required for the toxic activity of *Escherichia coli* hemolysin, Science 266 (1994) 1992–1996.
[29] J. Masin, M. Basler, O. Knapp, M. El-Azami-El-Idrissi, E. Maier, I. Konopasek, R. Benz, C. Leclerc, P. Sebo, Acylation of lysine 860 allows tight binding and cytotoxicity of *Bordetella* adenylate cyclase on CD11b-expressing cells, Biochemistry 44 (2005) 12759–12766.
[30] V. Herlax, L. Bakas, Acyl chains are responsible for the irreversibility in the *Escherichia coli* alpha-hemolysin binding to membranes, Chem. Phys. Lipids 122 (2003) 185–190.
[31] V. Herlax, S. Mate, O. Rimoldi, L. Bakas, Relevance of fatty acid covalently bound to *Escherichia coli* alpha-hemolysin and membrane microdomains in the oligomerization process, J. Biol. Chem. 284 (2009) 25199–25210.
[32] J.C. Karst, V.Y. Ntsogo Enguene, S.E. Cannella, O. Subrini, A. Hessel, S. Debard, D. Ladant, A. Chenal, Calcium, acylation, and molecular confinement favor folding of *Bordetella pertussis* adenylate cyclase CyaA toxin into a monomeric and cytotoxic form, J. Biol. Chem. 289 (2014) 30702–30716.
[33] D.P. O'Brien, S.E. Cannella, A. Voegele, D. Raoux-Barbot, M. Davi, T. Douche, M. Matondo, S. Brier, D. Ladant, A. Chenal, Post-translational acylation controls the folding and functions of the CyaA RTX toxin, Faseb. J. 33 (2019) 10065–10076.
[34] M. El-Azami-El-Idrissi, C. Bauche, J. Loucka, R. Osicka, P. Sebo, D. Ladant, C. Leclerc, Interaction of *Bordetella pertussis* adenylate cyclase with CD11b/CD18: role of toxin acylation and identification of the main integrin interaction domain, J. Biol. Chem. 278 (2003) 38514–38521.
[35] G. Karimova, J. Pidoux, A. Ullmann, D. Ladant, A bacterial two-hybrid system based on a reconstituted signal transduction pathway, Proc. Natl. Acad. Sci. U. S. A. 95 (1998) 5752–5756.
[36] C. Nicolai, F. Sachs, Solving ion channel kinetics with the QuB software, Biophys. Rev. Lett. 8 (2013) 191–211.
[37] N.P. Greene, A. Crow, C. Hughes, V. Koronakis, Structure of a bacterial toxin-activating acyltransferase, Proc. Natl. Acad. Sci. U. S. A. 112 (2015) E3058–E3066.
[38] P. Stanley, V. Koronakis, K. Hardie, C. Hughes, Independent interaction of the acyltransferase HlyC with two maturation domains of the *Escherichia coli* toxin HlyA, Mol. Microbiol. 20 (1996) 813–822.
[39] S. Pellett, R.A. Welch, *Escherichia coli* hemolysin mutants with altered target cell specificity, Infect. Immun. 64 (1996) 3081–3087.
[40] A. Ludwig, F. Garcia, S. Bauer, T. Jarchau, R. Benz, J. Hoppe, W. Goebel, Analysis of the in vivo activation of hemolysin (HlyA) from *Escherichia coli*, J. Bacteriol. 178 (1996) 5422–5430.
[41] C. Guzman-Verri, F. Garcia, S. Arvidson, Incomplete activation of *Escherichia coli* hemolysin (HlyA) due to mutations in the 3' region of hlyC, J. Bacteriol. 179 (1997) 5959–5962.